Journal of Engineering and Development, Vol. 12, No. 3, September (2008) ISSN 1813-7822

Behavior of Composite Beam with Partial Connection Under Flexural Wave Propagation

Asst. Lect. Hesham Abd AL-Latef Numan
Civil Engineering Department, College of Engineering
Al-Mustansiriya University, Baghdad, Iraq

Abstract

This research presents a theoretical study to the behavior of composite beam with partial connection under flexural wave propagation, connected together by stud shear connectors. Equilibrium and compatibility are satisfied for the forces and displacements at the assumed element.

As a result, five simultaneous differential equations with respect to x-axis and time (t), with different deflections and rotations in each element, taking into account slip occurring at the interface between elements, and entire effect of time by the method of characteristics with Laxwendroff solution. A computer program is written in (Visual Basic) to apply the suggested theoretical model.

الخلاصـــــة

يتضمن هذا البحث دراسة نظرية لتصرف العتبة المركبة ذات الترابط الجزئي تحت تأثير انتشار موجة الانحناء، المرتبطة معاً بالروابط القصية. معادلات التوازن والتوافق طبقت للقوى والإزاحات خلال عناصر الطبقتين.

تم التوصل إلى خمس معادلات بالنسبة للمحور السيني والزمن، مع اختلاف كل من التشوه والتدوير لكل عنصر، مع الأخذ بنظر الإعتبار الانزلاق الذي يحدث في السطح البيني بين العنصرين، وإدخال تأثير الزمن بواسطة نظرية الخصائص مع حل لكسوندروف. كتب البرنامج الحاسوبي بلغة (فيجيوال بيسك) لتطبيق النموذج النظري المفترض.

1. Introduction

The properties of each material differ from the properties of another material; thus there is no material that can provide all the structural requirements. This is the reason of using two or more materials and connecting them together in order to make full advantage of their properties in getting one structural element that uses the desirable properties of the materials. The advantageous characteristics of different materials are combined to produce a member with high carrying capacity. Then, the structural member of two or more materials is known as a composite member.

When successive dropping load is applied to an elastic body over a very short period and affect relatively long time, the response should be considered in terms of wave propagation theory. The problem of flexural wave's propagation in composite beams has not been extensively treated as the problems of longitudinal wave's propagation. This is due to the complexities involved in the propagation of flexural waves and their dispersive character.

Both components in a typical composite beam are usually connected together by shear connectors, all connectors are flexible (horizontal and vertical separation occur at the interface between elements), therefore partial interaction is always used in practice. The most widely used type of connectors is the headed stud, with a diameter ranging from (13-25) mm, and length ranging from (65-100) mm. The studs are attached to the steel member by an automatic stud-welding machine. There are two factors that influence the choice of stud diameter (d_S). One is the welding process, which becomes increasingly expensive and difficult for diameters exceeding (19mm), and the other is the thickness (t_f) of the plate or the flange to which the stud should be welded, especially when (d_S/t_f) is less than (2.7). The studs to be flexible are required to be made from steel with minimum elongation of (18%) and characteristic yield stress not less than (400N/mm^2).

2. Literature Review

Most researchers are neglected effect of shear deformation and rotatory inertia in the behavior of composite beam under flexural wave propagation; therefore, the solutions were lost accurate [1,2,3,4]. In this research is displaying of some research studied effect the two movements.

In 1921, Timoshenko [5] presented a theory which was then called by his name "Timoshenko theory", and was the only approximate theory that contains the essential features of the deep beam theory in simplified form. However, the Timoshenko equation for flexural wave propagation in beams can be presented as two second order partial differential equations:

$$\frac{\partial^2 \psi}{\partial x^2} - \frac{1}{C^2_P}\frac{\partial^2 \psi}{\partial t^2} = \frac{A.G.K_1}{E.I.}\left(\psi - \frac{\partial v}{\partial x}\right) \quad \text{.......} \quad (1)$$

$$\frac{\partial^2 \mathbf{v}}{\partial \mathbf{x}^2} - \frac{\mathbf{1}}{\mathbf{C}^2{}_\mathbf{S}} \frac{\partial^2 \mathbf{v}}{\partial \mathbf{t}^2} = \frac{\partial \psi}{\partial \mathbf{x}} \quad \textbf{(2)}$$

where:

$\mathbf{C_P} = \sqrt{\frac{\mathbf{E}}{\rho}}$, and $\mathbf{C_S} = \sqrt{\frac{\mathbf{K_1 G}}{\rho}}$

In 1971, Mandel, et. al. [6] combined Timeshenko theory of bending stress waves and the elementary theory to form a theory in which longitudinal and flexural stress waves were considered simultaneously. Using this theory, the effect of a rigid right angle joint on the transmission of flexural and longitudinal stress waves was determined .A test specimen was fabricated from Plexiglass ;it was L-shaped with strain gauges located on either side of the corner. Very good agreement between analysis and experiment substantiated the analysis developed in this work.

In 1988, Al-Mousawi, et. al. [7] presented various numerical solution methods for flexural wave propagation problems. The numerical methods considered are transform methods, finite element methods, finite difference methods and the method of characteristics.

Some numerical solutions have been obtained for a stepped beam using the method of characteristics and taking into account the effect of wave reflections. Several factors have been found to affect the level of stresses and the associated peak values, the main ones being the diameter ratio and the position of discontinuity. This work demonstrated that the use of the method of characteristics should be encouraged in finding solution for complicated flexural wave problems, where no other numerical solution methods can deliver satisfactory results. In the same year, Yiren [8] proposed a dynamic model for two-layered beams under impact loading. The model is based on Timoshenko beam theory but with accommodated interlayer slip. Different impact loads as well as different interfacial situations were investigated. The transient behavior of a two-layered beam was determined by the method of characteristic with Laxwendroff explicit dynamic governing equations.

In 1990, Abhyanker [9] studied numerical flexural wave propagation effects in a linearly elastic Timoshenko beam having both cross- sectional and material type of longitudinal discontinuities. A general formulation is presented which accounts for any number of discontinuities. For purposes of solution, the second order accurate explicit Maccormack's finite difference scheme is modified to account for the source term in Timoshenko beam equations and to include the effects of discontinuities. To demonstrate the effectiveness of the formulation and numerical procedure, some representative results are given for a single longitudinal discontinuity in cross-section and in material.

In 2001, Al-Amery and Hammed [10] produced a general formulation for the analysis of three-layered composite beam with partial interaction. Equilibrium and compatibility equations were reduced to a pair of differential equations of the fourth order in terms of slip in interface of (1) and (2) respectively.

3. Behavior of Composite Beam with Partial Connection under Flexural Wave Propagation

3-1 The Formulation

The simplest expression for displacement is to include the effect of transverse shear as well as the interlaminar slip, may be expanded into Taylor's series about y=0, Yiren [8], as follows:

$$\mathbf{u_c(x,y) = u_c(x) + \psi_c(x).y - \frac{2}{h}.[u]_{cs}.(y - \frac{h_s}{2})} \quad \text{..........} \quad \mathbf{(3)}$$

$$\mathbf{u_s(x,y) = u_s(x) + \psi_s(x).y - \frac{2}{h}.[u]_{cs}.(y + \frac{h_c}{2})} \quad \text{..........} \quad \mathbf{(4)}$$

And,

$$\mathbf{v_c(x,y) = v_c(x)} \quad \text{..........} \quad \mathbf{(5)}$$

$$\mathbf{v_s(x,y) = v_s(x)} \quad \text{..........} \quad \mathbf{(6)}$$

where:

h: is the total thickness of the composite element,

h_c: is the thickness of concrete slab,

h_s: is the thickness of steel beam and $h= h_c+ h_s$.

3-1-1 Equilibrium

The principle of virtual work for the present problem is written as:

$$\int_{t^*}^{t^\wedge}\int_{0}^{L}\Bigg[N_c.\frac{\partial\delta u_c}{\partial x}+N_s.\frac{\partial\delta u_s}{\partial x}+M_c.\frac{\partial\delta\psi_c}{\partial x}+M_s.\frac{\partial\delta\psi_s}{\partial x}-\frac{2}{h}.M^*.\frac{\partial\delta[u]_{cs}}{\partial x}$$

$$-Q_c.\delta\psi_c-Q_s.\delta\psi_s-\frac{2}{h}.Q.\delta[u]_{cs}+Q_c\frac{\partial\delta v_c}{\partial x}+Q_s\frac{\partial\delta v_s}{\partial x}\Bigg]$$

$$-\rho_c.b_c.\Bigg\{(h_c).\dot{u}_c(x).\delta\dot{u}_c(x)+\left(\frac{h_c.h_s}{2}\right).\dot{\psi}_c(x).\delta\dot{u}_c(x)+\left(\frac{h_c.h_s}{2}\right).\dot{u}_c(x).\delta\dot{\psi}_c(x)$$

$$+\left(\frac{h_c^{\ 3}+3.h_c.h_s^{\ 2}}{12}\right).\dot{\psi}_c(x).\delta\dot{\psi}_c-\left(\frac{h_c^{\ 3}}{6.h}\right).[\dot{u}]_{cs}.\delta\dot{\psi}_c(x)-\left(\frac{h_c^3}{6.h}\right).\delta[\dot{u}]_{cs}.\dot{\psi}_c(x)+$$

$$\left(\frac{h_c^{\ 3}}{3.h^2}\right).\delta[\dot{u}]_{cs}.[\dot{u}]_{cs}+(h_c).\dot{v}_c(x).\delta\dot{v}_c(x)\Bigg\}$$

$$-\rho_s.b_s.\Bigg\{(h_s).\dot{u}_s(x).\delta\dot{u}_s(x)-\left(\frac{h_c.h_s}{2}\right).\dot{\psi}_s(x).\delta\dot{u}_s(x)$$

$$-\left(\frac{h_c.h_s}{2}\right).\dot{u}_s(x).\delta\dot{\psi}_s(x)+\left(\frac{h_s^{\ 3}-3.h_c^3}{12}\right).\dot{\psi}_s(x).\delta\dot{\psi}_s(x)$$

$$-\left(\frac{h_s^3-6.h_c^2.h_s-3.h_c.h_s^2-3.h_c^3}{6.h}\right).[\dot{u}]_{cs}.\delta\dot{\psi}_s(x)$$

$$+\left(\frac{h_s^3}{3.h^2}\right).\delta[\dot{u}]_{cs}.[\dot{u}]_{cs}+\left(h_s\right).\dot{v}_s(x).\delta\dot{v}_s(x)+T.\delta[u]_{cs}-R\delta v_c-R\delta v_c\Bigg\}.dx.dt=0 \quad \ldots\ldots (7)$$

The axial force is a small quantity and negligible so that the axial displacement can be ignored and integrating equation (7) by parts using the variational principle.

3-1-2 Compatibility

The shear flow (T) is related to the interface slip$[u]_{cs}$ by the equation:

$$T = K_s.[u]_{cs} \quad \ldots\ldots (8)$$

The slip $[u]_{cs}$ at the interface between the concrete and steel, is shown in **Fig.(1)**. The relative deflection at interface of concrete and steel $(\nu)_{CS}$ is the relative displacement in y-direction of the initially adjacent particles, while the rotation $(\psi)_{cs}$ at the central line of the composite beam is defined as the relative displacement in x-direction of the initially adjacent particles, as shown in **Fig.(2)**.

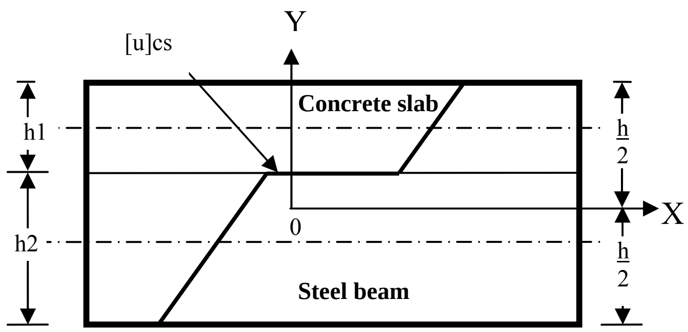

Figure (1) Coordinate system of composite beam

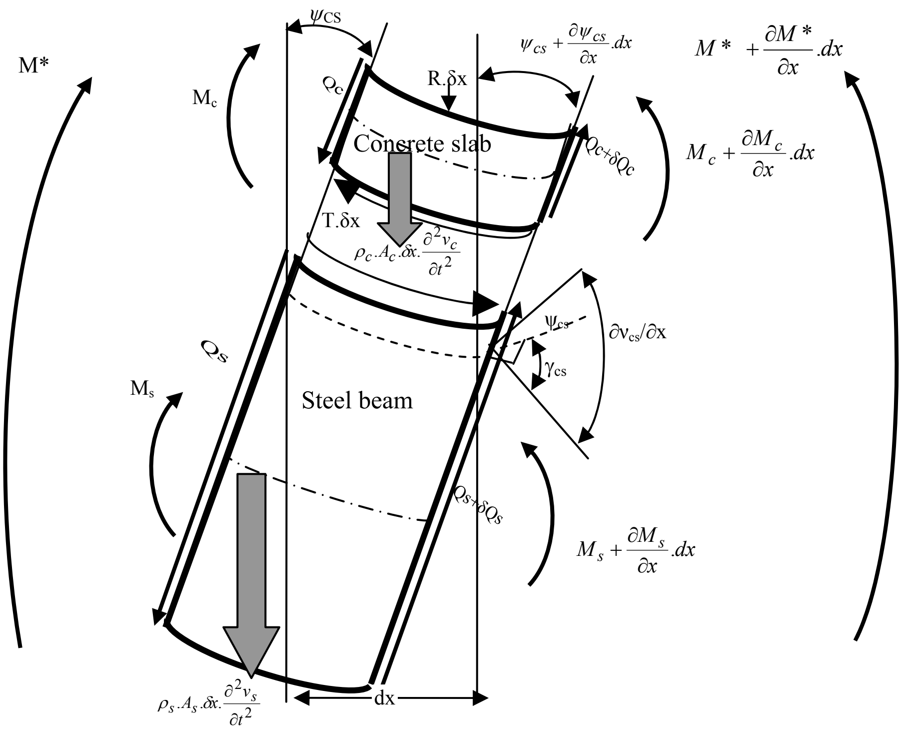

Figure (2) Timoshenko beam under rotation and inertia forces where central axis of each composite element, central line of composite element

The bending moments (M_C and M_S) are obtained by integrating the stresses, multiplied by ($y°_m$ and $y°_n$ respectively), (M*) is obtained by integrating the stresses multiplied by (y^*_m and y^*_n), (Q_c and Q_s) are obtained by integrating the shear stresses, over the cross section area of concrete slab and steel beam, denoted by (A_c) and (A_s). Hence:

$$\mathbf{M_c = \int \sigma_{x_c} . y^\circ_m . dA_c} \quad \text{.......... (9)}$$

$$\mathbf{M_s = \int \sigma_{x_s} . y^\circ_n . dA_s} \quad \text{.......... (10)}$$

$$\mathbf{M^* = \int \sigma_{x_c} . y^*_m . dA_c + \int \sigma_{x_s} . y^*_n . dA_s} \quad \text{.......... (11)}$$

$$\mathbf{Qc = \int \tau_{xy_c} . dA_c} \quad \text{.......... (12)}$$

$$\mathbf{Q_s = \int \tau_{xy_s} . dA_s} \quad \text{.......... (13)}$$

where:

$$\mathbf{\sigma_{x_c} = E_c . (y^\circ_m . \psi_{c,x} + y^\circ_n . \frac{2h_c^3}{h^4} [u]_{cs,x})} \quad \text{.......... (14)}$$

$$\sigma_{x_s} = E_s.(y^o_m.\psi_{s,x} + y^o_n.\frac{2h_s^3}{h^4}[u]_{cs,x}) \quad \text{.........} (15)$$

$$\tau_{xy_c} = K_1.G_c.\gamma_{o_c} \quad \text{.........} (16)$$

$$\tau_{xy_s} = K_1.G_s.\gamma_{o_s} \quad \text{.........} (17)$$

Substituting equations (14) and (15) into equations (9) to (11) and substituting equations (16) and (17) into equations (12) and (13) gives:

$$M_c = E_c.I_c.\frac{\partial \psi_c}{\partial x} - E_c.I_c.\frac{2.h_c^3}{h^4}.\frac{\partial [u]_{cs}}{\partial x} \quad \text{.........} (18)$$

$$M_s = E_s.I_s.\frac{\partial \psi_s}{\partial x} - E_s.I_s.\frac{2.h_s^3}{h^4}.\frac{\partial [u]_{cs}}{\partial x} \quad \text{.........} (19)$$

$$M^* = \left(E_c.I_c.\frac{\partial \psi_c}{\partial x} + E_s.I_s.\frac{\partial \psi_s}{\partial x}\right).e - \frac{2.e}{h}\left(E_c.I_c + E_s.I_s\right).\frac{\partial [u]_{cs}}{\partial x} \quad \text{.........} (20)$$

where:

$e = (h_c^3 + h_s^3)/h^3$

$$Q_c = K_1.b_c.G_c.h_c.\left(\frac{\partial v_c}{\partial x} - \psi_c - \frac{2}{h}.[u]_{cs}\right) \quad \text{.........} (21)$$

$$Q_s = K_1.b_s.G_s.h_s.\left(\frac{\partial v_s}{\partial x} - \psi_s - \frac{2}{h}.[u]_{cs}\right) \quad \text{.........} (22)$$

and,

$$Q = Q_c + Q_s \quad \text{.........} (23)$$

The basic equilibrium and compatibility equations give:

$$-E_c.I_c.\frac{\partial^2 \psi_c}{\partial x^2} + E_c.I_c.\frac{2.h_c^3}{h^4}.\frac{\partial^2 [u]_{cs}}{\partial x^2} - K_1.b_c.G_c.h_c.\frac{\partial v_c}{\partial x} + K_1.b_c.G_c.h_c.\psi_c$$
$$+ 2.K_1.b_c.G_c.\frac{h_c}{h}.[u]_{cs} + \rho_c.I_c.\frac{h_c^3 + 3.h_c.h_s^2}{12}.\ddot{\psi}_c(x)$$
$$-\rho_c.b_c.\frac{h_c^3}{6.h}.[\ddot{u}]_{cs} = 0 \quad \text{.........} (24)$$

$$-E_s.I_s.\frac{\partial^2\psi_s}{\partial x^2}+E_s.I_s.\frac{2.h_s^3}{h^4}.\frac{\partial^2[u]_{cs}}{\partial x^2}-K_1.b_s.G_s.h_s.\frac{\partial v_s}{\partial x}+K_1.b_s.G_s.h_s.\psi_s$$
$$+2.K_1.b_s.G_s.\frac{h_s}{h}.[u]_{cs}+\rho_s.b_s.\frac{h_s^3-3.h_c^2}{12}.\ddot{\psi}_s(x)$$
$$-\rho_s.b_s.(\frac{h_s^3-6.h_c^2.h_s-3.h_s.h_s^2-3.h_c^3}{6.h}).[\ddot{u}]_{cs}=0 \quad \ldots\ldots (25)$$

$$\frac{2}{h}.e.E_c.I_c.\frac{\partial^2\psi_c}{\partial x^2}+\frac{2.e}{h}.E_s.I_s.\frac{\partial^2\psi_s}{\partial x^2}-\frac{4.e}{h^2}.(E_c.I_c+E_s.I_s).\frac{\partial^2[u]_{cs}}{\partial x^2}$$
$$-\frac{2}{h}.K_1.b_c.G_c.h_c.\frac{\partial v_c}{\partial x}+2.K_1.b_c.\frac{h_c}{h}.\psi_c+\frac{4}{h^2}K_1.b_c.G_c.h_c.[u]_{cs}$$
$$-\frac{2}{h}.K_1.b_s.G_s.h_s.\frac{\partial v_s}{\partial x}+2.K_1.b_s.\frac{h_s}{h}.\psi_s+\frac{4}{h^2}.K_1.b_s.G_s.h_s.[u]_{cs}$$
$$-\rho_c.b_c.\frac{h_c^3}{6.h}.\ddot{\psi}_c(x)+\rho_c.b_c.\frac{h_c^3}{3.h^2}.[\ddot{u}]_{cs}$$
$$-\rho_s.b_s.(\frac{h_s^3-6.h_c^2.hs-3.h_c.h_s^2-3.h_c^3}{6.h}).\ddot{\psi}_s(x)$$
$$+\rho_s.b_s.\frac{h_s^3}{3.h^2}.[\ddot{u}]_{cs}+K_s.[u]_{cs}.=0 \quad \ldots\ldots (26)$$

$$-K_1.b_c.G_c.h_c.\frac{\partial^2 v_c}{\partial x^2}+K_1.b_c.G_c.h_c.\frac{\partial\psi_c}{\partial x}+2K_1.b_c.G_c.\frac{h_c}{h}[u]_{cs}=R \quad \ldots\ldots (27)$$

$$-K_1.b_s.G_s.h_s.\frac{\partial^2 v_s}{\partial x^2}+K_1.b_s.G_s.h_s.\frac{\partial\psi_s}{\partial x}+2K_1.b_s.G_s.\frac{h_s}{h}[u]_{cs}=R \quad \ldots\ldots (28)$$

3-2 Numerical Solution and Boundary Conditions

From equations (24) to (28) contain mix derivative of different types of variable and order with respect to x-axis and time. In the beginning, solution must be expressed in finite (central) difference from with respect to x-axis only so that all displacement derivatives with time are neglected (assuming the time in the beginning of loading is equal to zero). These equations contain derivatives of second order in x-axis ($[u],\psi,v$),so that three nodes are required to represent them in finite difference form and that requires to define one external node at each end of the beam to verify the substitution of the differential equations at the ends of the beam. Since each node is assigned five degrees of freedom, ten boundary conditions are required at each end. For example, the derivative of (v) at the node (n) can be expressed as:

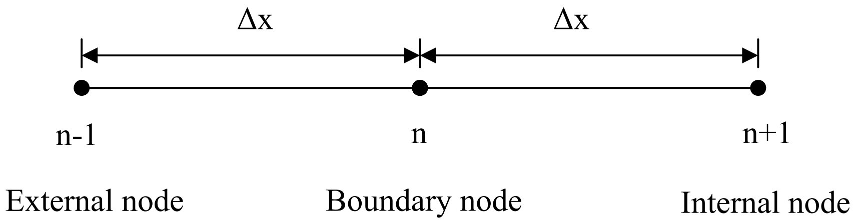

$$V_{cs\,n,x}=\frac{V_{cs\,n+1}+V_{cs\,n-1}}{2\Delta x}$$

$$V_{cs\,n,xx}=\frac{V_{cs\,n-1}+2V_{cs\,n}+V_{cs\,n+1}}{\Delta x^{2}}$$

in which (Δx) is the spacing between nodes.

To complete the set of algebraic equations, the boundary conditions for a simply supported beam of length (L) employed in this theory are: ($V_C=0$, $V_S=0$, $V_{C,\,xx}=0$, $V_{S,\,xx}=0$, $\psi_{C,\,x}=0$, $\psi_{S,\,x}=0$, $\psi_{c,\,xx}=0$, $\psi_{s,\,xx}=0$, $[u]_{CS,\,x}=0$, and $[u]_{CS,\,xx}=0$ *when x=0 and x= L*), and then entire effect of time representation by the method of characteristics with Laxwendroff explicit [8] dynamic governing equations (29) to (31).

$$S^*_{,t^*}= C_p.S^*_{,x}+Cs.S^*_{,x}+C_m \;\ldots\ldots (29)$$

$$S^\circ_{,t^*}= C_p.S^\circ_{,x}+Cs.S^\circ_{,x}+C_n \;\ldots\ldots (30)$$

$$[u]_{cs,\,t^*}=C_{p\,av.}\,[u]_{CS,\,x}+ C_{s\,av.}[u]_{CS,\,x}+ C_{av.} \;\ldots\ldots (31)$$

Solution of equation (29) to (31) at time ($t^*+\Delta t$) is expanded by Taylor's series:

$$S^{*t^*+\Delta t}=S^{*t^*}+\Delta t.\left[Cp_c.\frac{S^*_{n+1}-S^*_{n-1}}{2.\Delta x}+Cs_c.S^*_n+C_m\right]^{t^*}+\frac{\Delta t^2}{2}.$$

$$\left[Cp_c.Cp_c.\frac{S^*_{n+1}-2S^*_n+S^*_{n-1}}{\Delta x^2}+\right.$$

$$\left.(Cp_c.Cs_c+Cs_c.Cp_c).\frac{S^*_{n+1}-S^*_{n-1}}{2.\Delta x}+Cs_c.Cs_c.S^*_n+Cs^*.C_m\right]^{t^*} \;\ldots\ldots (32)$$

$$S^{\circ t^*+\Delta t}=S^{\circ t^*}+\Delta t.\left[Cp_s.\frac{S^\circ_{n+1}-S^\circ_{n-1}}{2.\Delta x}+Cs_s.S_{sn}+C_n\right]^{t^*}$$

$$+\frac{\Delta t^2}{2}.\left[Cp_s.Cp_s.\frac{S^\circ_{n+1}-2S^\circ_n+S^\circ_{n-1}}{\Delta x^2}+(Cp_s.Cs_s+Cs_s.Cp_s).\right.$$

$$\left.\frac{S^{\circ}_{n+1}-S^{\circ}_{n-1}}{2.\Delta x}+Cs_s.Cs_s.S^{\circ}_n+Cs_s.C_n\right]^{t*} \qquad (33)$$

$$[u]^{t*+\Delta t}_{cs}=[u]^{t*}_{cs}+\Delta t.\left[Cp_{av.}.\frac{[u]_{cs\ n+1}-[u]_{cs\ n-1}}{2.\Delta x}+Cs_{av.}.[u]_{cs.n}+C_{av.}\right]^{t*}$$

$$+\frac{\Delta t^2}{2}.\left[Cp_{av.}.Cp_{av.}.\frac{[u]_{cs\,n+1}-2[u]_{cs\,n}+[u]_{cs\,n-1}}{\Delta x^2}+(Cp_{av.}.Cs_{av.}+Cs_{av.}.Cp_{av.}).\right.$$

$$\left.\frac{[u]_{cs\ n+1}-[u]_{cs\ n-1}}{2.\Delta x}+Cs_{av}.Cs_{av}.[u]_{csn}+Cs_{av}.C_{av.}\right]^{t*} \qquad (34)$$

where:

$C_m=Cs_c/Cp_c.\ R$,
$C_n=Cs_s/Cp_s.R$,
$C_{av.}=Cs_{av.}/Cp_{av.}.R$ and,
$R=q+P_e$

Dropping load (P) can be idealized as uniformly distributed load (P_e=P/Δx) applied over a single node spacing, (q is the live load and dead load of concrete and steel beam),(Δt is the difference time between two drops loading and assumed equal). Increment of time (Δt) is add, to give new results of displacements. The process continued, until arriving to final time of dropping load.

4. Conclusions

1. The Present approach, which has five degrees of freedom, gives reasonable prediction to the behavior along the length of the simply supported beam and can be used for any type of dropping load condition.
2. Finite difference (central) and the method of characteristics by Laxwendroff solution representation is efficient for analysis of simply supported beam and gives a good saving in computer, time and effort.
3. A more accurate result is achieved when using the layered approach.
4. Approximate relationship between slip and the applied dropping load present along the whole length of simply supported can be noticed (in **Appendix (A)**).
5. Composite material is able to transmit and reflect the waves and give small movements (slip, deflection and rotation) because the characteristics of different material are combined to produce a member with high carrying capacity.

5. References

1. Miller, A. K., and Adams, D. F., ***"An Analytic Means of Determining the Flexural and Torisonal Resonant Frequencies of Generally Beams"***, Journal Sound Vibration, Vol. 41, 1975.

2. Warburton, G. B., ***"The Dynamical Behavior of Structures"***, 2nd Edition, 1976.

3. Doyle, J. F., and Kamle, S., ***"An Experimental Study of the Reflection and Transmission of Flexural Waves at Discontinuities"***, Journal Applied Mechanic, Vol. 52, 1985.

4. Vinson, J. R., and Sierakowski, R. L., ***"The Behavior of Structures Composed of Composite Martinus Nijhoff, Dordrechant"***, The Netherlands, 1986.

5. Timoshenko, S. P., ***"On the Transverse Vibrations of Bars of Uniform Cross-Section"***, Phil. Mag. Ser. 7, 1921.

6. Mandal, J. A., Mathur, R. K., and Chang Y. C., ***"Stress Waves at Rigid Right Angle Joint"***, Journal of Engineering Mechanics, Vol. 4, 1971.

7. Al-Mousawi, M. M., Harrison, H. R., and Ghosh, S. K., ***"On Numerical Solution Methods for Flexural Waves in Stepped Beams"***, International Journal of Impact Engineering, Vol. 7, No. 3, 1988.

8. Yiren, X., ***"Behavior of a Two-layered Beam under Impact Loading"***, International Journal of Impact Engineering, Vol. 7, No. 4, 1988.

9. Abhyankar, N. S., ***"Flexural Waves in Beams with Geometrical and Material Longitudinal Discontinuities"***, International Journal of Impact Engineering, Vol. 9, No. 2, 1990.

10. Al-Amery, R. I. M., and Hammed, S. A., ***"Structural Behavior of Multi-Layered Composite Beam"***, Proceeding of the First National Conference in Civil Engineering, Iraq, 2001.

Notations and Suffixes

A	Cross sectional area.
b	Effective width of the beam.
C_p,C_s	Bending wave velocity and shear wave velocity, respectively.
C_m,C_n,$C_{av.}$	Constant as defined
d_s	Outside diameter of headed stud.
E	Modulus of elasticity.
e	Thickness factor.
f_{cu}	Cubic compressive strength of concrete.
fy	Specified yield strength of steel.
G	Shear modulus of the beam.
I	Moment of inertia of section about centroidal axis.
K_1	Shear correction factor.
K_s	Modulus of shear connection per unit length.
L	Span length of composite beam.
M	Moment with respect to the central line x=0.
M*	Sum of moments of layers with respect to each layer's central axis.
N	Axial force.
n	Number of shear connectors in row.
P	A concentrated load (dropping load).
Q	Applied shear force.
q	Applied load per unit length of the beam.
R	External load per unit length of the beam.
S*	Variable is equal to deflection and rotation of concrete.
S°	Variable is equal to deflection and rotation of steel.
t*, t^	Time at the beginning and final of loading.
t_f	Thickness of steel flange.
T	Longitudinal shear force per unit length at the interface.
u	Axial displacement.
[u]	Slip at the interface.
v	Poisson's ratio.
X,Y	Shorter overall dimension of rectangular part of cross section and longer
y°_m,y°_n	Representing depth from central line of composite beam to upper edge of
y^*_m,y^*_n	Lever arm of composite couple.
δ	Infinitesimal increment.
v	Deflection displacement.
ρ	Density of the beam.
ψ	Rotation of the beam.
σ_x	Normal stress.
τ_{xy}	Normal strain.
γ_0	Infinitesimal angle of shearing effect.
Δ	Small but finite dimension.

Suffixes

c,s,cs	Concrete slab, steel beam and composite beam, respectively.
$\cdot$	Differential with time.
$\cdot\cdot$	Double differential with time.
,x	Differential with x.
$\partial^2/\partial t^2$	Double partial differential with time.
$\partial/\partial x$	Partial differential with x.
$\partial^2/\partial x^2$	Double partial differential with x.

Appendix (A)

Example of Composite Floor Beam

A typical composite floor beam section with dimensions shown in **Fig.(A-a)**, is composed of concrete slab and steel beam. The beam has span (L=10000 mm), and it is subjected to the successive dropping load of (200 kN) at middle span, dropping load is stopping when arriving to forty seconds of time. The other properties are given in **Table (A-1)**, and shown in **Fig.(A-b)**.

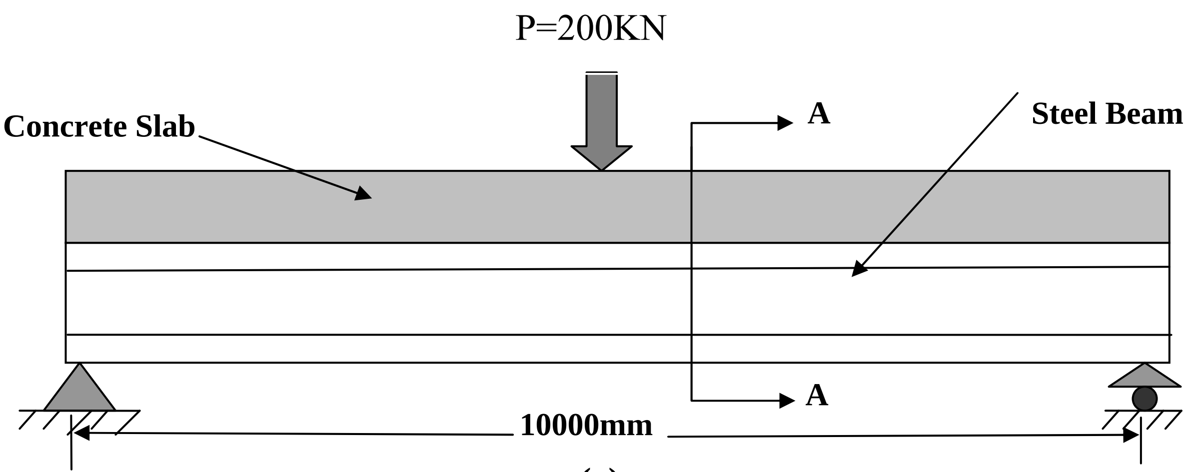

(a)

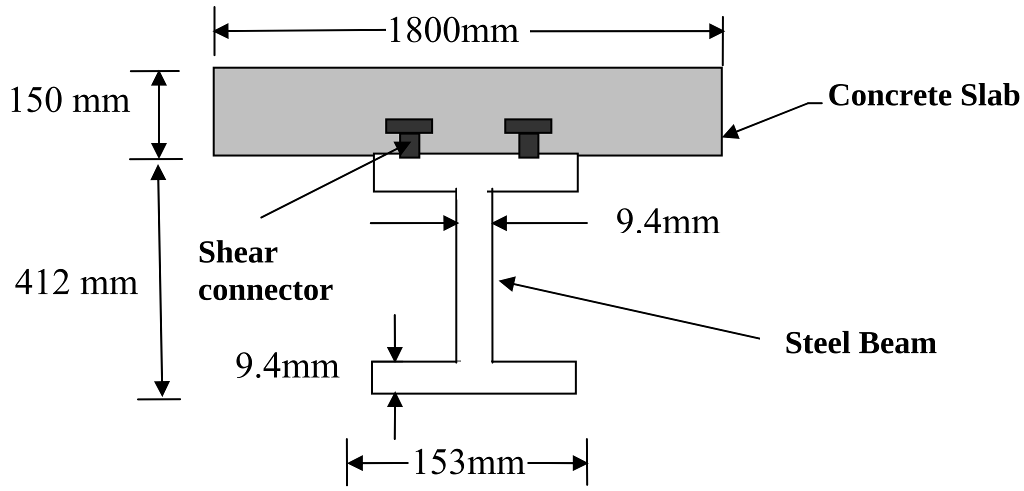

Figure (A) (a) Simply supported beam subjected to the successive dropping load at mid- span
(b) Section (A-A) at the beam

Table (A-1) Composite floor beam material properties

Material	Property	Value
Concrete slab	Characteristic cube strength fcu (N/mm^2)	30
	Modulus of elasticity Ec (kN/mm^2)	26.70
	Density ρ_c (kN/mm^3).	0.000000025
	Shear modulus Gc (kN/ mm^2).	11.608
Steel beam (I-section)	Characteristic yield strength fy (N/mm^2)	250
	Modulus of elasticity Es (kN/mm^2)	200
	Density ρ_s (kN/mm^3)	0.000000075
	Poisson's ratio v_s	0.30
Shear connectors (headed stud)	Diameter (mm) x Height (mm)	19x100
	Spacing (mm)	250
	Number of studs in row (n)	2
	Shear stiffness of connector (kN/mm)	180

Inputs Data for Example of Composite Floor Beam

h_s=412 mm

b_c=1800 mm

h_c=150 mm

b_f =153 mm

t_f =9.4 mm

b_w =9.4 mm

h_w =393.2 mm

E_c=26.70 kN/mm^2

E_s=200 kN/mm^2

K_1=0.8333

G_c=11.608 kN/mm^2

v_s= 0.3

ρ_c=0.000000025 kN/mm^3

ρ_s= 0.000000075 kN/mm^3

K_s=180 kN/mm

P= 200 kN

L= 10000 mm

Δt =0.01sec

T_1(final time) = 40 sec

N(No. of node) =25

L.L=4.79 $*10^{-6}$ kN/mm^2

Results of Example Composite Floor Beam in Figures (4, 5 and 6)

Distance along the beam (mm)	Slip Velocity (m/sec)
0	0.0161
1250	0.01325
2500	0.00755
3750	0.00185
5000	0
6250	-0.00185
7500	-0.00755
8750	-0.01325
10000	-0.0161

Distance along the beam (mm)	Rotation Velocity (rad/sec)
0	0.0051
1250	0.00425
2500	0.00255
3750	0.00085
5000	0
6250	-0.00085
7500	-0.00255
8750	-0.00425
10000	-0.0051

Distance along the beam (mm)	Deflection Velocity (m/sec)
0	0
1250	-0.00525
2500	-0.0115
3750	-0.01775
5000	-0.025
6250	-0.01775
7500	-0.0115
8750	-0.00525
10000	0

Figure (4) shows slip velocity which occurs along the span of composite floor beam. In the left support, the maximum slip velocity value is (0.0161m/sec). This value decreases slowly until approach zero (at 0.5L from left support). Then, the slip velocity increases at opposite direction until it reaches maximum value at right support (the same value in the left support).

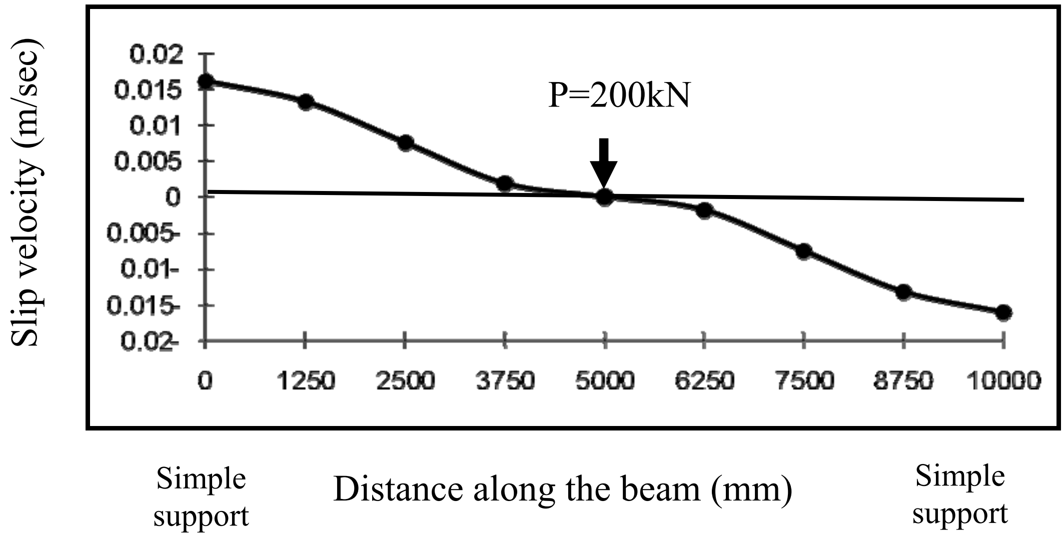

Figure (4) Slip velocity variation along the simply supported beam at time 40sec

Figure (5) shows deflection velocity which occurs along the span of composite floor beam. In the left support, the deflection velocity value is equal to zero and decreases rapidly until it approaches maximum value at middle span (0.025m/sec). Then, the curve slowly increases until they approach zero at right su]

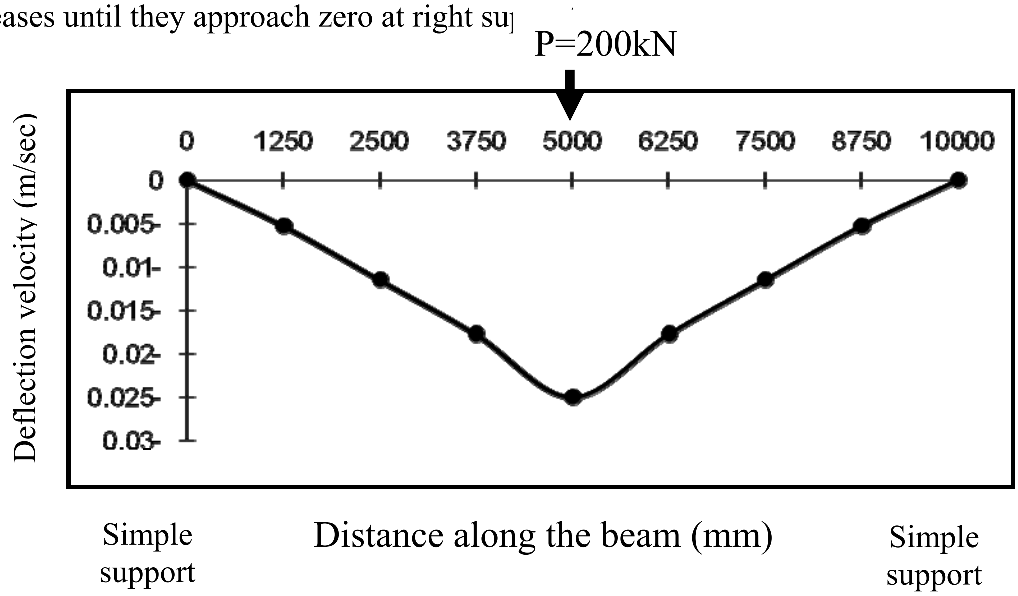

Figure (5) Deflection velocity variation along the simply supported beam at time 40sec

Figure (6) shows rotation velocity which occurs along the span of composite floor beam. In the left support, the maximum rotation velocity value is (0.0051m/sec).This value decreases slowly until approach zero (at 0.5.L from left support). Then, the rotation velocity increases at opposite direction until it reaches the maximum value at right support (the same value in the left support).

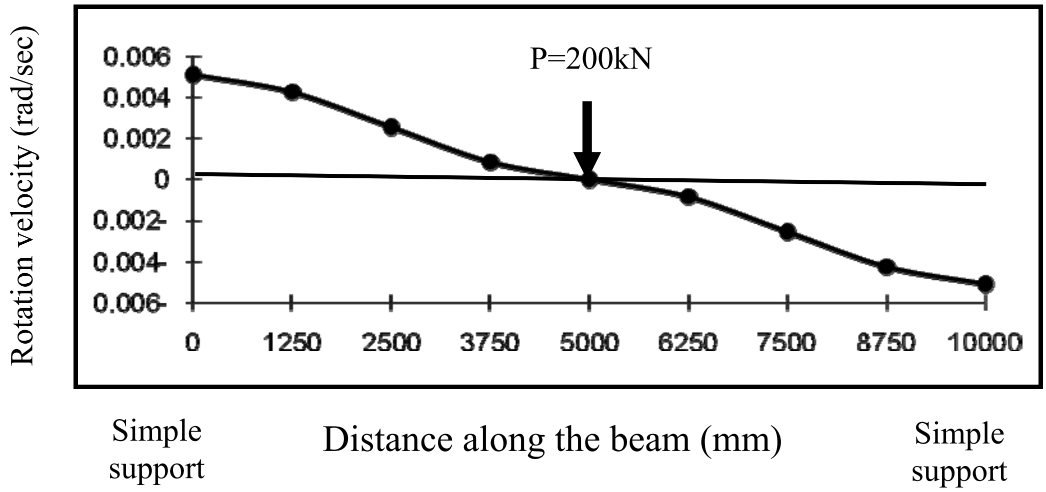

Figure (6) Rotation velocity variation along the simply supported beam at time 40sec

Appendix (B)

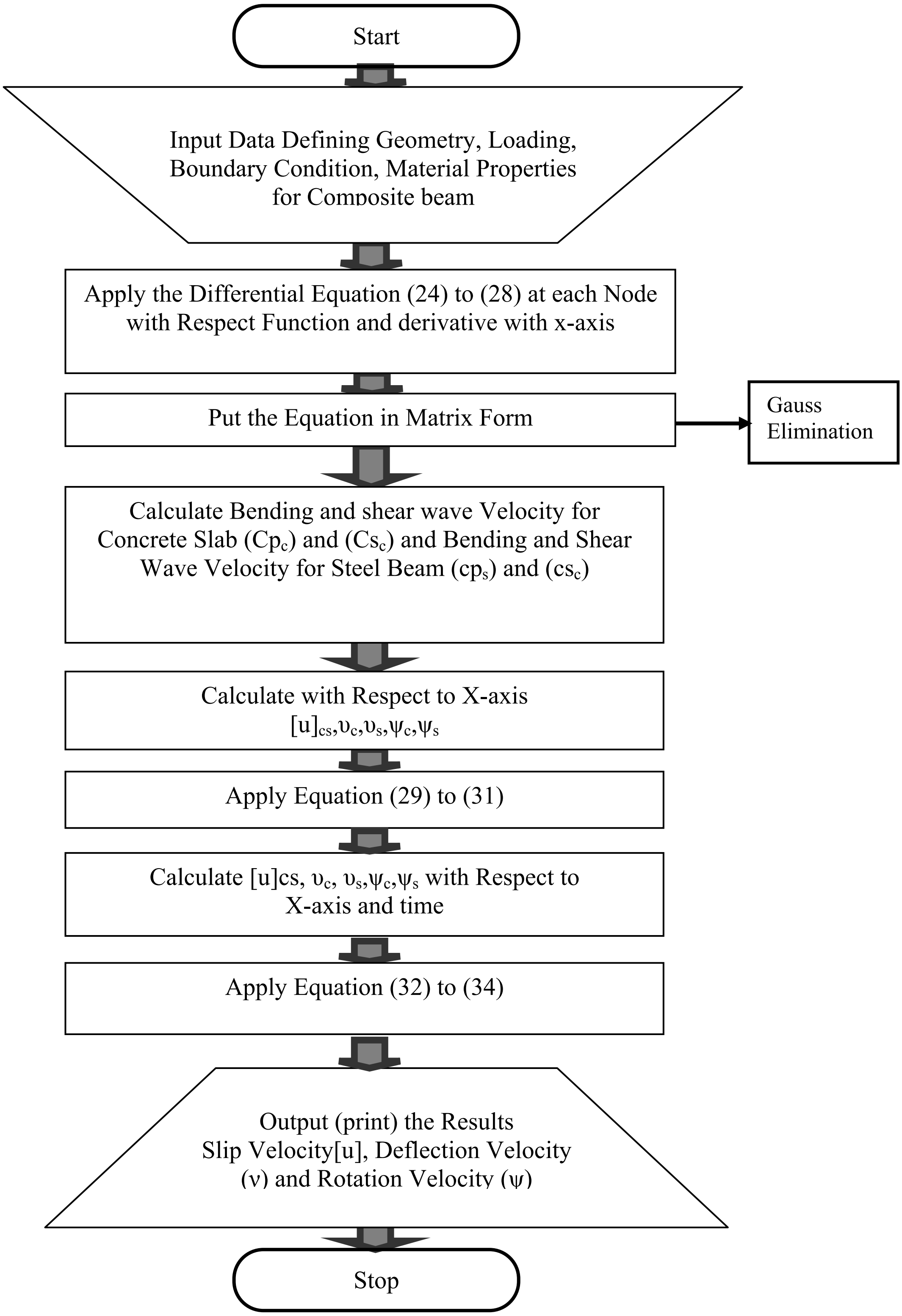

Flowchart showing composite beam under successive dropping load

Appendix (C)

Example of Two- Layered Beam System

A typical two layers beam , with the same material and properties (steel and steel), as used by Yiren [8] .The beam of span (200 mm) is subjected to a point load at the middle span of (200 kN) at final time equal to twenty micro seconds, as shown in **Fig.(7-a)**. The other properties are given **Table (C-1)**, and shown in **Fig.(7-b)**. A convergence study has been carried out on this beam in order to indicate the right number of nodes to be taken for numerical solution from which an acceptable result can be obtained.

Table (C-1) Material properties

Material	Property	Value
Steel beam	Characteristic yield strength fy (N/mm^2).	250
	Young's modulus of elasticity Es (kN/mm^2).	200
	Poisson's ratio v_s.	0.27
	Density ρ_s (kN/mm^3).	0.000000075
Glue	Shear modulus of adhesive Ga (N/mm^2).	4.00
	Adhesive thickness η (mm).	0.02

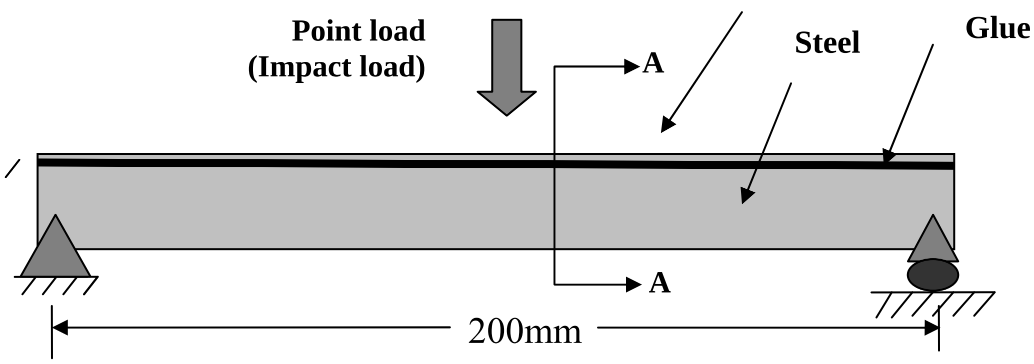

(a)

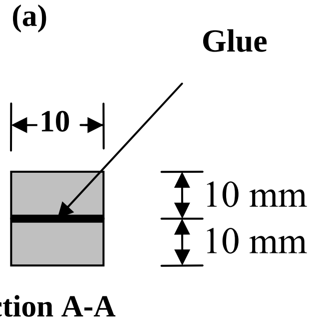

(b)

Figure (7) (a) A Typical two-layer beam system (steel and steel connected by glue) [8]
(b) Section at the beam

Table (C-2) shows a comparison between Yiren's solution [8] and numerical solution presented in this study. It can be seen that, the difference between these solutions is within (13%) when the number of nodes is (10). This difference is reduced to (10.66%) when the number of nodes becomes (25) and it becomes (9%) at 45 nodes. This illustrates that numerical solution can be used even at small intervals between adjacent nodes with acceptable tolerance. Therefore, the total number of nodes, used to apply the current numerical solution, is (25) node. This is obtained by dividing the beam into twenty-three equal elements.

Table (C-2) Comparison between numerical solution for the suggested model and Yiren's Solution

Number of nodes	Numerical Solution for Suggested Models			Yiren's Solution
	45	25	10	
Slip Velocity at left hand support (m/sec)	0.327	0.332	0.339	0.3

General examination of **Fig.(8)** at time of twenty micro seconds shows that the maximum slip velocity occurs at left support and decreases slowly along half length of the beam until it approaches zero at (0.5L from the left support). Then, the slip increases at opposite direction until it reaches a maximum value at the right support. Hence, close agreement at both ends of the beam has been obtained.

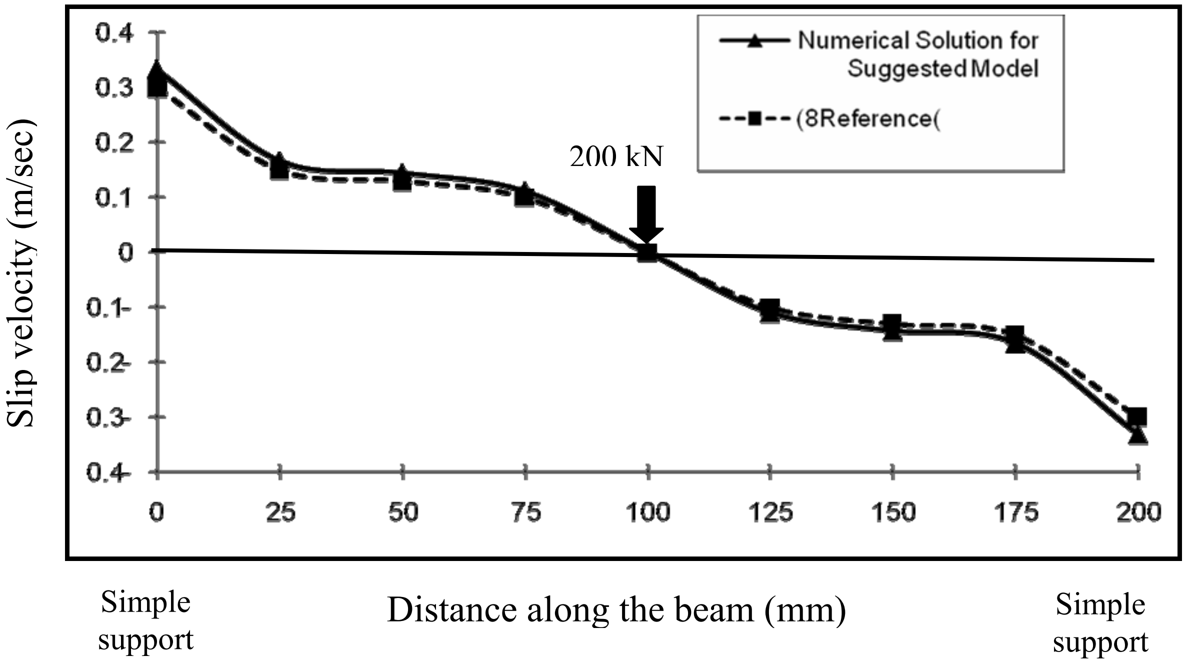

Figure (8) Slip velocity variation along the simply supported beam at time 20 μs